Mueller, P. R., & Wold, B. (1989) *Science 246*, 780-786.
Nussinov, R. (1989) *J. Biomol. Struct. Dyn. 6*, 985-1000.
Nussinov, R., Sarai, A., Smythers, G. W., & Jernigan, R. L. (1988) *J. Biomol. Struct. Dyn. 6*, 543-562.
Oka, Y., & Thomas, C. A. (1987) *Nucleic Acids Res. 15*, 8877-8898.
Otting, G., Grutter, R., Leupin, W., Minganti, C., Ganesh, K. N., Sproat, B. S., Gait, M. J., & Wuthrich, K. (1987) *Eur. J. Biochem. 166*, 215-220.
Pinnavaia, T. J., Miles, H. T., & Becker, E. D. (1975) *J. Am. Chem. Soc. 97*, 7198-7200.
Pluta, A. F., Kaine, B. P., & Spear, B. B. (1982) *Nucleic Acids Res. 10*, 8145-8154.
Pluta, A. F., Dani, G. M., Spear, B. B., & Zakian, V. A. (1984) *Proc. Natl. Acad. Sci. U.S.A. 81*, 1475-1479.
Price, C. M., & Cech, T. R. (1989) *Biochemistry 28*, 769-774.
Raguhuraman, M. K., & Cech, T. R. (1990) *Nucleic Acids Res. 18*, 4543-4552.
Richards, E. J., & Ausubel, F. M. (1988) *Cell 53*, 127-136.
Roberts, L. (1988) *Science 240*, 982-983.
Saenger, W. (1984) *Principles of Nucleic Acid Structure*, Springer-Verlag, New York.
Schein, C. H. (1990) *Biotechnology 8*, 308-317.
Sen, D., & Gilbert, W. (1988) *Nature 334*, 364-366.
Sen, D., & Gilbert, W. (1990) *Nature 344*, 410-414.
Shippen-Lentz, D., & Blackburn, E. H. (1989) *Mol. Cell. Biol. 9*, 2761-2764.
Sundquist, W. I., & Klug, A. (1989) *Nature 342*, 825-829.
Tibanyenda, N., DeBruin, S. H., Haasnoot, C. A. G., van der Marel, G., van Boom, J. H., & Hilbers, C. W. (1984) *Eur. J. Biochem. 139*, 19-27.
Watson, J. D. (1972) *Nature, New Biol. 239*, 197-201.
Wemmer, D. E., Chou, S. H., Hare, D. R., & Reid, B. R. (1985) *Nucleic Acids Res. 13*, 3755-3772.
Williamson, J. R., Raghuraman, M. K., & Cech, T. R. (1989) *Cell 59*, 871-880.
Wolk, S. K., Hardin, C. C., Germann, M. W., van de Sande, J. H., & Tinoco, I., Jr. (1988) *Biochemistry 27*, 6960-6967.
Zimmerman, S. B., Cohen, G. H., & Davies, D. R. (1975) *J. Mol. Biol. 92*, 181-192.

Intramolecular Triplex Formation of the Purine·Purine·Pyrimidine Type†

Fu-Ming Chen
Department of Chemistry, Tennessee State University, Nashville, Tennessee 37209-1561
Received November 5, 1990; Revised Manuscript Received January 31, 1991

ABSTRACT: Six octadecamers with hairpin motifs have been synthesized and investigated for possible intramolecular triplex formation. Electrophoretic, hypochromic, and CD evidence suggest that d(CCCCTTTGGGGTTTGGGG) and d(GGGGTTTGGGGTTTCCCC) can form G·G·C intramolecular triplexes via double hairpin formation in neutral solutions, presumably with the terminal G tract folding back along the groove of the hairpin duplex. In contrast, d(GGGGTTTCCCCTTTGGGG) and the three corresponding 18-mers containing one G and two C tracts each forms a single hairpin duplex with a dangling single strand. The design of the sequences has led to the conclusion that the two G tracts are antiparallel to each other in such a triplex. Magnesium chloride titrations indicate that Mg^{2+} is not essential for such an intramolecular triplex formation. The main advantage of our constructs when compared to the intermolecular triplex formation is that the shorter triplex stem can be formed in a much lower DNA concentration. The merit of G·G·C triplex, in contrast to that of C^+·G·C, lies in the fact that acidic condition is not required in its formation and will, thus, greatly expand our repertoire in the triplex strategy for the recognition and cleavage of duplex DNA. Spectral binding studies with actinomycin D (ACTD) and chromomycin A_3 (CHR) as well as fluorescence lifetime measurements with ethidium bromide (EB) suggest that although hairpin duplexes bind these drugs quite well, the intramolecular triplexes bind poorly. Interestingly, the binding densities for the strong-binding hairpins obtained from Scatchard plots are about one ACTD molecule per oligomeric strand, whereas more than two drug molecules are found in the case of CHR, in agreement with the recent NMR studies indicating that CHR binds to DNA in the form of a dimer.

Homopurine–homopyrimidine sequences have been mapped to several sites in the regulatory regions of eukaryotic genes that are found to be hypersensitive to single-strand-specific nucleases such as S1 (Larsen & Weintraub, 1982; Nickol & Felsenfeld, 1983; Elgin, 1984). These sequences have been suspected to exhibit unusual DNA structures, as they are known to undergo a transition in plasmids to an underwound state under conditions of moderately acidic pH and negative supercoiling (Wells et al., 1988, and references cited therein). Recent studies on these systems (Htun & Dahlberg, 1988; Johnston, 1988) appear to support a model consisting of a triple-stranded (pyr·pur·pyr) plus a single-stranded structure called H-DNA (Lee et al., 1984; Lyamichev et al., 1986).

Triplex formation has also been exploited as a strategy for DNA recognition and site-specific double-helical cleavage (Mosher & Dervan, 1987; Strobel et al., 1988; DeDoan et al., 1987; Praseuth et al., 1988; Povsic & Dervan, 1989; Maher et al., 1989; Francois et al., 1989; Horne & Dervan, 1990; Perrouault et al., 1990) and has generated considerable excitement in recent years. Such a strategy utilizes, for example, homopyrimidine oligodeoxyribonucleotides with EDTA·Fe attached to a single position to form pyr·pur·pyr triplexes and cleave the duplex DNA at those recognition sites. Studies on

† This work was supported by USPHS Grant CA-422682 and by a subproject of MBRS Grant S06RR0892.

0006-2960/91/0430-4472$02.50/0

the location and asymmetry of the cleavage pattern revealed that the homopyrimidine–EDTA probes bind in the major groove parallel to the homopurine strand of Watson–Crick double-helical DNA. Recent NMR studies on the pyr·pur·pyr triplex formation have largely confirmed these structural details (De los Santos et al., 1989; Rajagopal & Feigon, 1989; Pilch et al., 1990; Umemoto et al., 1990) and further established the Hoogsteen base-pairing scheme for the third strand. Such a triplex technique to isolate large segments of genomic DNA for mapping and sequencing may have important implication for human genetics, as is dramatically illustrated by the most recent demonstration of the site-specific cleavage of a yeast chromosome by oligonucleotide-directed triple-helix formation (Strobel & Dervan, 1990).

In contrast to the pyr·pur·pyr triplexes, studies on the pur·pur·pyr triplexes have been relatively rare (Marck & Thiele, 1978; Broitman et al., 1987; Cooney et al., 1988; Letai et al., 1988). Of particular interest is the work of Kohwi and Kohwi-Shigematsu (1988) in which they applied a fine-structure mapping technique to supercoiled plasmid DNA to study the unusual DNA structure adopted by the poly(dG)·poly(dC) sequence under torsional stress at pH 5 and various ionic conditions. The results led to the suggestion that the poly(dG)·poly(dC) stretch is folded into halves from the center of the sequence to form either a triplex consisting of poly(dG)·poly(dG)·poly(dC) in the presence of Mg^{2+} with the two dG strands running antiparallel to each other or a triplex consisting of poly(dC^+)·poly(dG)·poly(dC) in the absence of Mg^{2+} with one of the dC strands protonated and running parallel to the dG strand. These results demonstrate that pyr·pur·pyr and pur·pur·pyr triplexes can exist in the same system under different conditions.

Despite the obvious advantage of not requiring acidic conditions for such a pur·pur·pyr triplex formation, no attempt has thus far been made to investigate its potential in the strategy for the site-specific recognition and cleavage of duplex DNA. In an effort to gain further insights into various aspects of triplex formation and to test the existing structure models, especially those of the pur·pur·pyr type, oligonucleotides with hairpin structural motifs were synthesized and investigated for possible intramolecular triplex formation.

Six 18-mers, d(CCCCTTTCCCCTTTGGGG) (to be designated as C/C/G), d(CCCCTTTGGGGTTTCCCC) (C/G/C), d(GGGGTTTCCCCTTTCCCC) (G/C/C), d(CCCCTTTGGGGTTTGGGG) (C/G/G), d(GGGGTTTCCCCTTTGGGG) (G/C/G), and d(GGGGTTTGGGGTTTCCCC) (G/G/C), were synthesized for this purpose. Those containing one tract of C and two tracts of G will be collectively designated as C1G2, whereas the oligomers containing two tracts of C and one tract of G will be denoted as C2G1. Electrophoretic and CD evidence is presented to demonstrate the existence of G·G·C intramolecular triplexes in two of the oligomers studied. Spectral measurements (absorbance, CD, and fluorescence lifetime) on drug binding were made to render further support for the existence of such a conformation. Actinomycin D (ACTD) and chromomycin A_3 (CHR) were chosen for their guanine specificity and their differing binding modes, intercalative and groove binding, respectively. Ethidium bromide (EB) was chosen for the ability to greatly enhance its fluorescence upon DNA binding.

Rationale for the Choice of Oligomers and Some Predictions. These oligomers were chosen for their ability to form single and, in some cases, double hairpins for possible intramolecular triplex formation. Our constructs have the advantage over intermolecular triplex formation in that shorter stem sequences and lower DNA concentrations can be used since the interacting components are always in close proximity. On the basis of the knowledge that in pyr·pur·pyr triplexes the Hoogsteen strand is parallel to the purine whereas in pur·pur·pyr triplexes it is antiparallel unless the syn conformation is used for the third strand, the following predictions can be made.

(1) *If the two G tracts are required to be antiparallel in a G·G·C triplex formation, then d(CCCCTTTGGGGTTTGGGG) and d(GGGGTTTGGGGTTTCCCC) will likely form intramolecular triplexes while d(GGGGTTTCCCCTTTGGGG) and the three C2G1 octadecamers will not.* In the C/G/G or G/G/C 18-mer, a hairpin can form between the proximal G and C tracts while the terminal G tract can fold back along the major groove to form an intramolecular triplex with antiparallel polarity to the duplex G tract. The G/C/G oligomer, however, is not expected to form such a triplex, since the two G tracts will be parallel upon the double hairpin formation. The formation of an intramolecular triplex will result in a 4-base-triad stem and two 3-base loops with an electrophoretic mobility expected to be slightly faster than a decameric duplex. In contrast, the formation of a single hairpin with a dangling single strand will result in a mobility approximately that of a 13- or 14-mer duplex.

(2) *In slightly acidic conditions, d(CCCCTTTCCCCTTTGGGG) and d(GGGGTTTCCCCTTTCCCC) are expected to form C^+·G·C triplexes whereas d(CCCCTTTGGGGTTTCCCC) is not.* The C/C/G and G/C/C 18-mers may form intramolecular triplexes such that the terminal C tract can be protonated and folded back along the major groove of the Watson–Crick hairpin duplex to form Hoogsteen base pairs with the G tract in a parallel fashion. The C/G/C 18-mer, however, is not expected to form an intramolecular triplex even in acidic conditions, as both C tracts will be antiparallel to the G tract upon hairpin formation.

(3) *Reduced affinities for drugs are expected for triplexes* as the presence of a third strand in the major groove will block the access to this groove and enhance the rigidity of DNA, hindering both intercalative and groove binding.

Materials and Methods

Oligonucleotides were synthesized with a Biosearch 8600 DNA synthesizer with use of β-cyanoethyl phosphoramidite chemistry. The crude oligomer was purified by a strong anion-exchange (SAX) HPLC and repurified by reversed-phase HPLC chromatography as detailed earlier (Chen, 1988). The purified and lyophilized oligomers were dissolved in 10 mM Tris(hydroxymethyl)aminomethane hydrochloride (Tris-HCl) buffer of pH 8 containing 0.1 M NaCl. All experiments were carried out in this buffer. Since oligomers rich in guanine are notorious in aggregate formation, these stock solutions were first heated in boiling water for about 4 min and then cooled back to ambient temperatures. Concentrations of these oligomers (per nucleotide) were determined with absorbances at 260 nm after melting, with use of extinction coefficients obtained through nearest-neighbor approximation with mono- and dinucleotide values tabulated in Fasman (1975).

Absorption spectra were measured with a Cary 210 spectrophotometric system. CD spectra were measured by a Jasco J-500A recording spectropolarimeter at appropriate temperatures, with use of water-jacketed cylindrical cells. Spectral titrations were carried out at 18.5 °C for ACTD and 25 °C for CHR. Due to their relative slow rates of association, a 20-min waiting period was allowed after each addition.

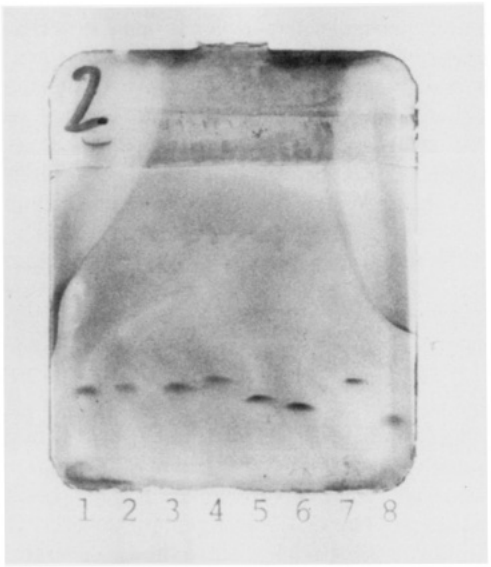

FIGURE 1: Comparison of electrophoretic mobilities of oligonucleotides on a 20% polyacrylamide PhastGel at 14 °C and 200 V with 75 Vh run time. PhastGel native buffer strips containing 0.25 M Tris at pH 8.8 were used, and the gels were prerun for 150 Vh prior to loading. The loading concentrations are in the range of 0.8–1.2 mM nucleotide. The gel was developed with silver staining. Lane 1: d-(CATGGCCATG). Lane 2: d(CCCCTTTGGGGTTTCCCC). Lane 3: d(GGGGTTTCCCCTTTCCCC). Lane 4: d-(CCCCTTTCCCCTTTGGGG). Lane 5: d-(CCCCTTTGGGGTTTGGGG). Lane 6: d-(GGGGTTTGGGGTTTCCCC). Lane 7: d-(GGGGTTTCCCCTTTGGGG). Lane 8: d(CCCCTTTGGGG).

ACTD, CHR, and EB were purchased from Sigma. The extinction coefficients used for drug concentration determination are 24 500 M^{-1} cm^{-1} at 440 nm for ACTD, 10 000 M^{-1} cm^{-1} at 400 nm for CHR, and 5850 M^{-1} cm^{-1} at 480 nm for EB. Thermal melting profiles of oligomers and their drug–DNA mixtures were carried out by monitoring absorbances at 275 nm and collecting data every 15 s with an Apple II microcomputer. A heating rate of 0.5 °C/min was maintained by a Neslab RTE-8 refrigerated circulating bath and an EPT-4RC temperature programmer. Numerical differentiations were performed to obtain differential melting profiles from which melting temperatures were deduced.

Fluorescence lifetime measurements were carried out with an SLM48000 multifrequency spectrometer at room temperatures with use of the phase/modulation techniques. An excitation wavelength of 510 nm and a long-pass filter of 550 nm were employed. The software provided by the manufacturer was used for the lifetime resolution analysis. Gel electrophoresis was run with a PhastSystem with 20% polyacrylamide gels and silver staining.

Results

Electrophoretic Mobilities of d(GGGGTTTGGGGTTTCCCC) and d(CCCCTTTGGGGTTTGGGG) Are Significantly Faster Than d(GGGGTTTCCCCTTTGGGG). Electrophoretic mobilities of all six 18-mers along with a self-complementary decamer d(CATGGCCATG) and an 11-mer with hairpin motif d(CCCCTTTGGGG) are compared in Figure 1. It is immediately apparent that the electrophoretic mobilities of C/G/G (lane 5) and G/G/C (lane 6) are considerably faster than those of G/C/G (lane 7) and the three C2G1 octadecamers (lanes 2–4). Furthermore, the decameric duplex d(CATGGCCATG) (lane 1) is found to move somewhat slower than C/G/G and G/G/C but faster than G/C/G. Also noteworthy is the fact that an 11-mer with the basic hairpin motif d(CCCCTTTGGGG) (lane 8) exhibits a single electrophoretic band with considerably faster mobility than a decameric duplex, suggesting that a hairpin with a 3-base loop predominates over an intermolecular duplex containing a bulge, thus ensuring negligible contributions from intermolecular multiplexes in oligomers studied in this work. The greater electrophoretic mobilities of G/G/C and C/G/G when compared to G/C/G are consistent with the expectation that they form G·G·C intramolecular triplexes via double hairpin formation, whereas G/C/G and the C2G1 oligomers only form single hairpins at pH 8.

CD Evidence Supports Intramolecular Triplex Formation in d(GGGGTTTGGGGTTTCCCC) and d(CCCCTTTGGGGTTTGGGG). To see if the faster moving oligomers exhibit distinct spectral characteristics, CD measurements of the six 18-mers were made and the results for the C1G2 oligomers are compared in Figure 2A. The CD spectra of the two 18-mers with adjacent G tracts are clearly different from that of the oligomer with the central C tract juxtaposed by two terminal G tracts. The outstanding feature of the C/G/G and G/G/C spectra is the prominent presence of a negative maximum at 278 nm, which is ostensibly absent in the G/C/G oligomer. The presence of this negative band in poly(dG)·poly(dC) has previously been identified to be the consequence of intermolecular G·G·C triple helix formation (Marck & Thiele, 1978; Thiele et al., 1978). Thus, the CD results support the notion that the former two 18-mers are capable of forming intramolecular triplexes. In contrast, the three C2G1 octadecamers at pH 8 exhibit very similar CD characteristics with broad CD bands having maxima around 270 nm and sizable positive intensities at 278 nm, as shown in Figure 2C. The CD features of the G/C/C oligomer are very similar to those of C/G/C and are not shown.

The presence of ordered structures for these oligomers is evidenced by the exhibited strong CD intensities and their gross temperature dependence with cooperative melting behaviors. Temperature-dependent CD spectra for the C/G/G oligomer are shown in Figure 2B. In addition to the dramatic intensity reduction at 260 nm around 60 °C, the concomitant disappearance of the 278-nm negative band is particularly noted. It is also worth mentioning the presence of approximate isoelliptic points around 246 and 270 nm, suggestive of a nearly two-state transition. Very similar features are exhibited by the G/G/C oligomer. The thermal-dependent CD characteristics for the C2G1 oligomers are represented by C/G/C in Figure 2D, which shows strong intensity reductions around 260 nm and the presence of an approximate isoelliptic point around 246 nm, as the temperature increases.

Melting Characteristics of the Oligomers. Characteristic melting profiles of these oligomers are represented in Figure 3 by C/G/G and C/C/G along with d(CCCCTTTGGGG) and d(CCCCGGGG). The greater thermal stability of the hairpin-forming oligomers as compared to the dimeric duplex d(CCCCGGGG) is immediately apparent. Although appreciable hyperchromic effects are seen in the premelting region (presumably the consequence of dimeric duplex melting) for C/C/G and d(CCCCTTTGGGG), a monophasic (except for a slight increase in absorbance below 10 °C) and more cooperative transition is exhibited by C/G/G. The nearly two-state transition for C/G/G is consistent with the presence of an isoelliptic point in the temperature-dependent CD spectra. Melting temperatures and the corresponding extinction coefficient changes per nucleotide at three different wavelengths are tabulated in Table I. The fact that all six 18-mers melt at temperatures closer to that of d-(CCCCTTTGGGG) ($t_m \sim 68$ °C) but considerably higher

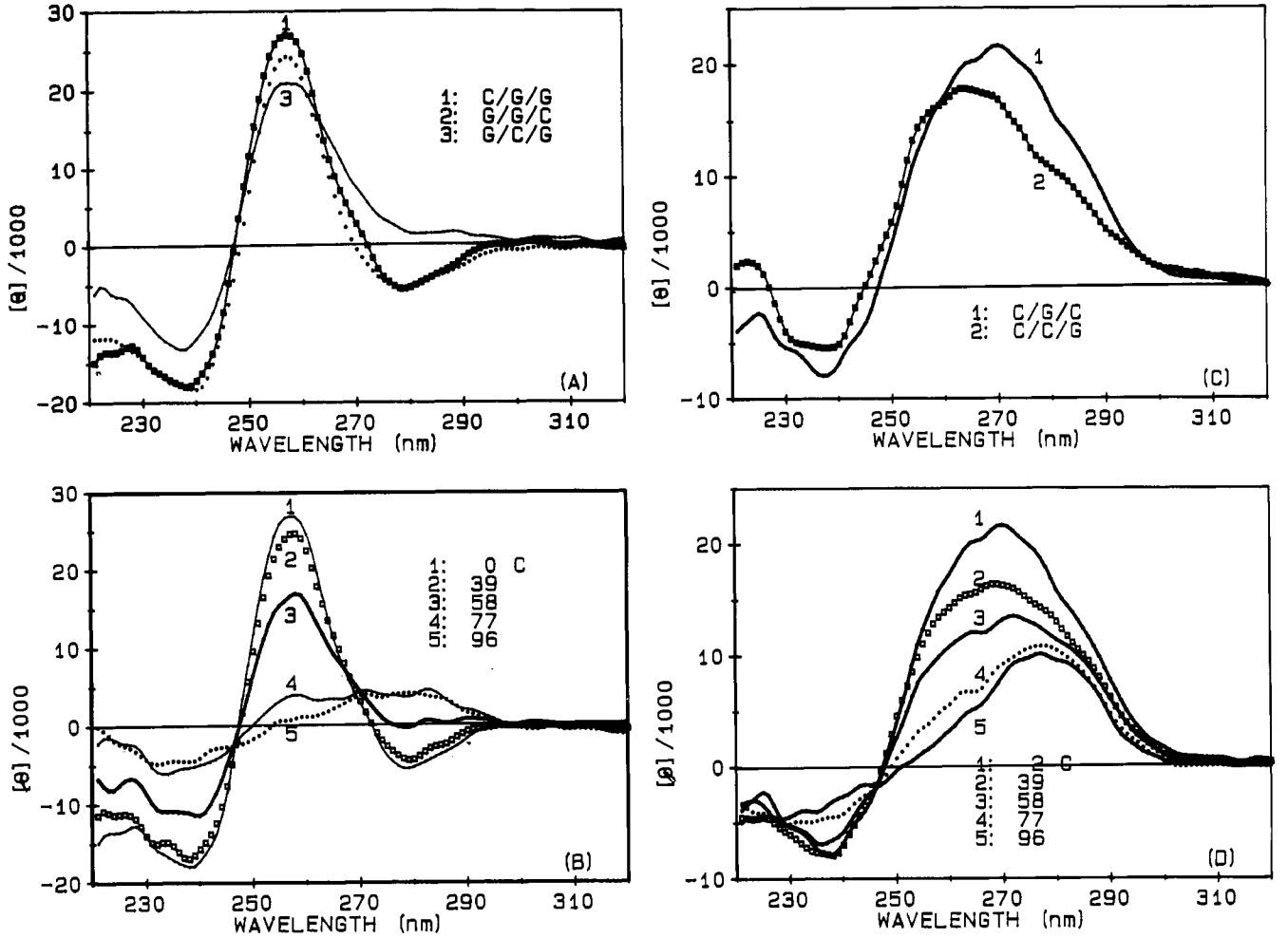

FIGURE 2: (A) Comparison of CD spectra at 2 °C for the C1G2 oligomers, d(CCCCTTTGGGGTTTGGGG) (□), d(GGGGTTTGGGGTTTCCCC) (···), and d(GGGGTTTCCCCTTTGGGG) (—). (B) Temperature-dependent CD spectra of d(CCCCTTTGGGGTTTGGGG). (C) Comparison of CD spectra of d(CCCCTTTGGGGTTTCCCC) (—) and d(CCCCTTTCCCCTTTGGGG) (□) at 2 °C. (D) CD spectra of d(CCCCTTTGGGGTTTCCCC) at some representative temperatures. CD measurements were made with 40 μM nucleotide solutions in a 2-cm cylindrical cell. The molar ellipticities were calculated with $[\theta] = 100\theta/lm$, where θ is the measured ellipticity in degrees, l is the pathlength in centimeters, and m is the concentration in moles per liter.

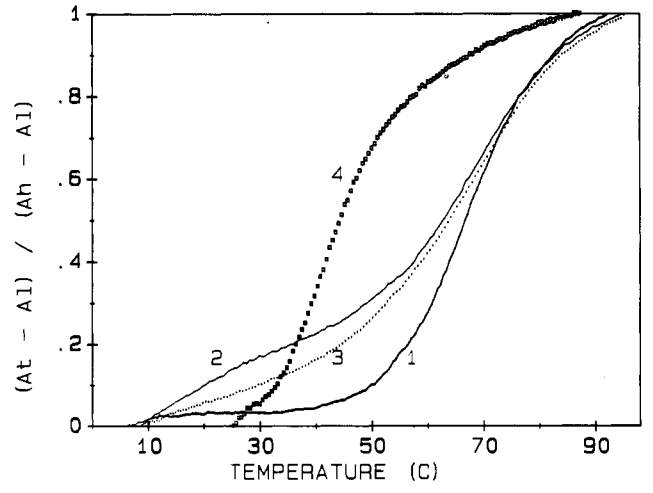

FIGURE 3: Representive melting profiles of 40 μM nucleotides in pH 8 Tris buffer containing 0.1 M NaCl: d(CCCCTTTGGGGTTTGGGG) (1); d(CCCCTTTCCCCTTTGGGG) (2); d(CCCCTTTGGGG) (3); and (CCCCGGGG) (4). Al, Ah, and At are absorbances at low (~3 °C), high (~97 °C), and t temperatures, respectively.

than that of dimeric duplex d(CCCCGGGG) (t_m ~ 40 °C) is consistent with the hairpin formation of these oligomers. The significantly lower melting temperatures exhibited by G/G/C and G/C/C as compared to the other four 18-mers further underscore the sequence effects on structural stability.

Table I: Melting Characteristics of Selected Oligomers

oligomer	t_m (°C)[a]	Δε- (300 nm)[b]	Δε- (285 nm)	Δε- (270 nm)
d(GGGGTTTGGGGTTTCCCC)	56	135	1085	840
d(CCCCTTTGGGGTTTGGGG)	64	150	1160	820
d(GGGGTTTCCCCTTTGGGG)	69	358	1210	990
d(GGGGTTTCCCCTTTCCCC)	55	88	925	1145
d(CCCCTTTGGGGTTTCCCC)	63	88	883	1065
d(CCCCTTTCCCCTTTGGGG)	68	113	853	998
d(CCCCTTTGGGG)	68	98	763	1295

[a] The estimated errors in melting temperatures are ±1 °C. [b] Difference extinction coefficients (between 97 and 3 °C) are in the unit of M^{-1} cm^{-1} (nucleotide).

Of particular interest is the relative hyperchromic effects upon melting. The two triplex-forming oligomers G/G/C and C/G/G consistently exhibit smaller extinction coefficient changes than those of G/C/G, especially at 300 and 270 nm. This is in apparent contrast to the general expectation that triplex formation will likely exhibit a greater hypochromic effect (and hyperchromic effect on melting) than that of duplex formation, as is the case in the pyr·pur·pyr triplexes. Interestingly, however, the smaller hyperchromic effects exhibited by G/G/C and C/G/G oligomers in comparison to G/C/G is not inconsistent with the notion of G·G·C triplex formation of these two 18-mers. Indeed, in contrast to poly(U·A·U),

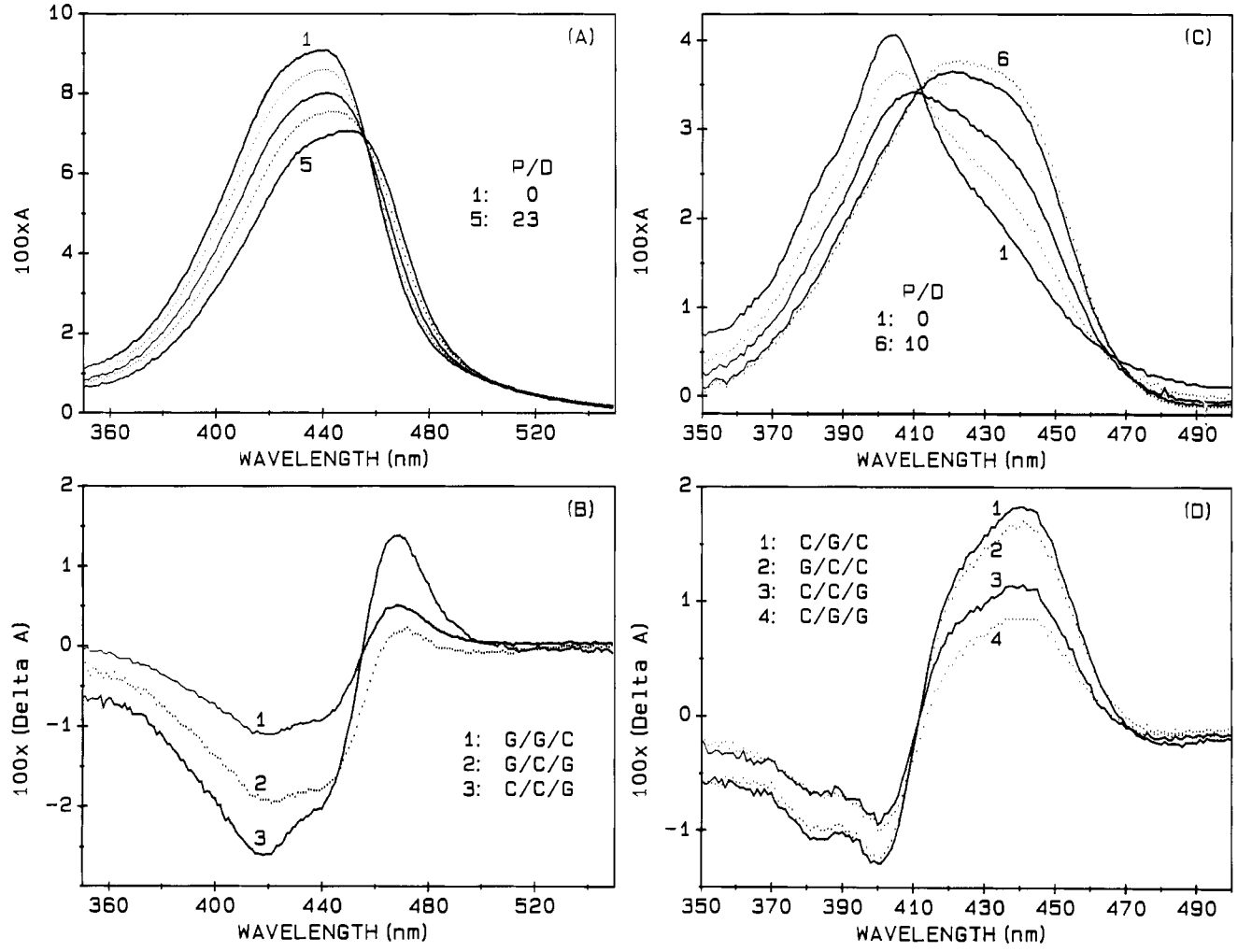

FIGURE 4: (A) Representative absorption spectra in the titration of ACTD with d(GGGGTTTCCCCTTTCCCC) at 18.5 °C. [ACTD] is normalized to 3.74 μM, and spectra with P/D values of 0, 3.4, 7.7, 13, and 23 are shown. (B) Comparison of difference spectra ((ACTD + DNA) − ACTD) for oligomers d(GGGGTTTGGGGTTTCCCC) (1), d(GGGGTTTCCCCTTTGGGG) (2), and d(CCCCTTTCCCCTTTGGGG) (3), with P/D ratios of approximately 19 except for that of spectrum 2, which is about 2-fold larger. (C) Spectral titrations of CHR with DNA as typified by d(CCCCTTTGGGGTTTCCCC) at 25 °C and the corresponding P/D values of 0, 1.6, 3.2, 4.8, 6.3, and 10, with [CHR] normalized to 3.9 μM. (D) Comparison of difference absorption spectra ((CHR + DNA) − CHR) for oligomers d(CCCCTTTGGGGTTTCCCC) (1), d(GGGGTTTCCCCTTTCCCC) (2), d(CCCCTTTCCCCTTTGGGG) (3), and d(CCCCTTTGGGGTTTGGGG) (4) for P/D values of approximately 10.

poly(A·A·U) triplex had been found to be hyperchromic relative to its poly(A·U) and poly(A) precursors (Broitman et al., 1987). It is also interesting to note in passing that the hyperchromic effects exhibited by the C2G1 oligomers are larger than the C1G2 oligomers at 270 nm but are smaller at 300 and 285 nm, likely the consequence of differing base compositions of these two series.

d(GGGGTTTGGGGTTTCCCC) and d(CCCCTTTGGGGTTTGGGG) Bind Weakly to Both Intercalator Actinomycin D and Groove-Binder Chromomycin A_3. Free ACTD exhibits a broad absorption band with a maximum around 440 nm. Upon DNA binding, strong hypochromic effects occur around 420 nm with concomitant appearance of weaker hyperchromic effects around 470 nm. Typical absorption spectral characteristics of ACTD during a titration are exemplified by G/C/C in Figure 4A. A clean isosbestic point is apparent at 455 nm, suggestive of a two-state event. The extent of hypochromic effects at 420 nm can, thus, be used as qualitative measures of ACTD binding affinity for various oligomers, provided the same D/P ([drug]/[DNA]) ratios are maintained. Such a comparison was made, and the results are shown in Figure 4B as difference spectra for P/D ratios of around 18 and an ACTD concentration of 3.7 μM. It is evident that the C2G1 oligomers, as represented by C/C/G, have stronger binding affinity for ACTD than the C1G2 oligomers. Significantly, G/C/G exhibits considerably stronger binding than G/G/C and C/G/G in the C1G2 series. These qualitative results are confirmed by binding constants deduced from Scatchard plots, which are summarized in Table II along with the chromomycin results to be described shortly. The binding constants for the C2G1 oligomers are seen to be around 2 μM^{-1} and the binding densities approximately one drug molecule per oligomer strand. Surprisingly, the ACTD

Table II: Comparison of Drug Binding Parameters[a]

	ACTD		CHR	
oligomer	K (μM^{-1})	n (per strand)	K	n
d(GGGGTTTGGGGTTTCCCC)	<0.1		<0.1	
d(CCCCTTTGGGGTTTGGGG)	<0.1		<0.1	
d(GGGGTTTCCCCTTTGGGG)	0.7		0.4	
d(GGGGTTTCCCCTTTCCCC)	2.5	1.1	2.5	2.6
d(CCCCTTTGGGGTTTCCCC)	1.7	1.3	3.8	3.4
d(CCCCTTTCCCCTTTGGGG)	2.1	1.4	0.3	

[a] The estimated errors for K and n are ±0.2 μM^{-1} and ±0.1, respectively.

binding affinities of some of the hairpin duplexes are stronger than that of poly(dG)·poly(dC), with binding constants comparable to those of dimeric duplexes containing the strong-binding dG-dC sequence (Chen, 1988). The ACTD binding order can, thus, be summarized as C/C/G ≅ C/G/C ≅ G/C/C > G/C/G > C/G/G ≅ G/G/C.

Chromomycin A_3 requires the presence of divalent cations such as Mg^{2+} for its DNA binding. It exhibits an absorbance maximum at 405 nm in the absence of DNA. A bathochromic shift is associated with its DNA binding to result in hyperchromic effects around 440 nm and concomitant hypochromic effects around 400 nm, yielding an isosbestic point at 412 nm. These effects are revealed more clearly in a typical titration for the C/G/C oligomer as shown in Figure 4C. Again, the extent of these hypochromic and hyperchromic effects can give qualitative indications as to the relative binding affinity of this drug to various oligomers. Absorbance difference spectra for some oligomers are shown in Figure 4D. Similar to the ACTD results, the CHR binding affinities of the C1G2 oligomers are seen to be much weaker than those of the C2G1 oligomers. Contrary to the nearly identical binding affinity for ACTD with the C2G1 oligomers, however, some significant differences were found in the case of CHR. Although C/C/G still exhibits stronger binding than C/G/G and G/G/C, it shows significantly weaker CHR binding affinity when compared to G/C/C and C/G/C. These facts are further supported by binding constants deduced from Scatchard plots, as tabulated in Table II. Binding of CHR to C/C/G is shown to be an order of magnitude weaker than C/G/C and G/C/C. It is also interesting to note that although the binding constants for the strong CHR binding oligomers exhibit the same order of magnitude binding constant as ACTD, the binding densities are roughly twice as high, i.e., more than two drug molecules per oligomer strand. These results coupled with the CD spectral measurements (not shown) suggest the following binding order for CHR: C/G/C ≳ G/C/C > C/C/G ≅ G/C/G > C/G/G > G/G/C.

Representative Scatchard plots for both CHR and ACTD are shown in Figure 5. It is immediately apparent that the G·G·C-forming oligomers bind much more weakly to ACTD or CHR than the other 18-mers. The plots for the stronger binding oligomers are seen to be reasonably well fitted by linear least squares.

Fluorescence Lifetime Measurements Also Suggest Weaker Ethidium Binding Abilities of G/G/C and C/G/G. Ethidium bromide exhibits a fluorescence lifetime of 1.8 ns in buffer solutions. Its lifetime increases more than 10-fold to around 22 ns upon intercalative binding to DNA. There is also evidence that external binding via electrostatic interaction results in a lifetime of approximately 10 ns. Fluorescence lifetime measurements were, thus, carried out to investigate the extent of ethidium binding to various oligomers. The phase/modulation technique was used for these measurements. Quantitative results can be obtained by numerically analyzing the measured frequency-dependent phase and/or modulation for their lifetime distribution. By utilizing the fact that the fluorescence lifetimes for the free and the intercalated ethidium are 1.8 and 21.7 ns, respectively, lifetime analyses were made by fixing one of the components to be 1.8 ns in the two-component analysis, whereas 1.8 and 21.7 ns were fixed in the three-component resolution. The results are shown in Table III. The relative contribution of the 1.8-ns lifetime for the unbound drug in each oligonucleotide solution can, thus, indicate the relative binding affinity. It is seen that C/G/G and G/G/C oligomers exhibit the largest 1.8-ns contributions of

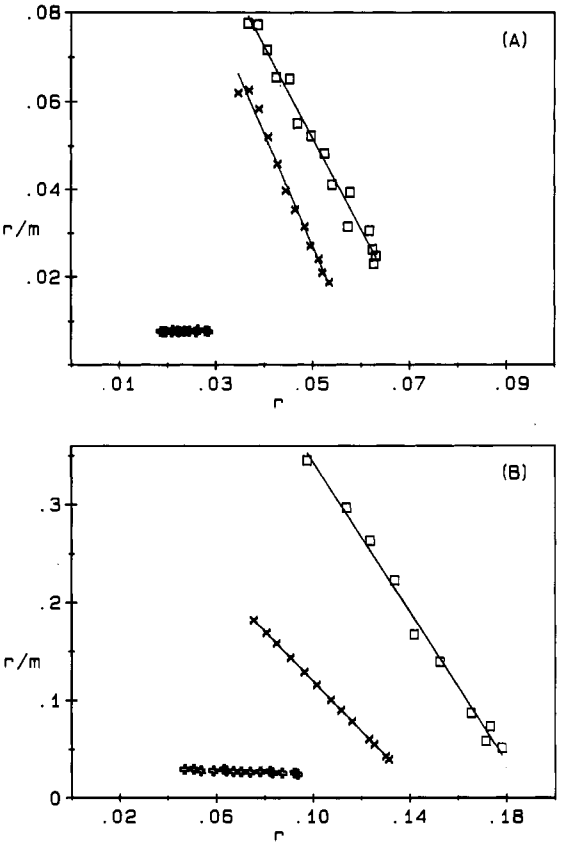

FIGURE 5: (A) Representative Scatchard plots in the titration of ACTD with d(GGGGTTTCCCCTTTCCCC) (×), d(CCCCTTTCCCCTTTGGGG) (□), and d(GGGGTTTGGGGTTTCCCC) (+) at 18.5 °C and pH 8, 0.1 M NaCl. Absorbance differences between 427 and 480 nm have been used to construct the Scatchard plots. Nearly identical extinction coefficients for the bound drugs were obtained for the first two oligomers via extrapolation from the 1/[DNA] plots, and their average was used for the G/G/C plot in which such an extrapolation was not feasible due to weak binding. (B) Representative Scatchard plots on the titration of CHR with d(CCCCTTTGGGGTTTCCCC) (□), d(GGGGTTTCCCCTTTCCCC) (×), and d(CCCCTTTGGGGTTTGGGG) (+) at 25 °C and pH 8, 0.1 M NaCl. Scatchard plots are constructed with absorbance differences between 400 and 440 nm. Nearly identical extinction coefficients for the bound drugs were obtained for the two strong-binding oligomers via extrapolation from the 1/[DNA] plots, and their average was used for the C/G/G plot in which such an extrapolation was not feasible due to weak binding.

all the oligomers studied, with the former exhibiting a weaker binding affinity. Results of these comparisons establish the ethidium binding order as C/C/G > G/C/G ≳ C/G/C ≳ G/C/C > G/G/C > C/G/G.

Discussion and Conclusion

The electrophoretic mobilities of d(CCCCTTTGGGGTTTGGGG) and d(GGGGTTTGGGGTTTCCCC) are found to be only slightly faster than that of a decameric duplex but sigificantly faster than that of d(GGGGTTTCCCCTTTGGGG), which in turn moves measurably slower than a dodecameric duplex (not shown). These results are consistent with the expectation of intramolecular G·G·C triplex formation for the two fast-moving 18-mers via double hairpin formation, presumably with the terminal G tract folding back along the major groove of the hairpin duplex with antiparallel polarity to the central G tract. Such a conformation will result in a 4-base-triad stem and two 3-base loops. Assuming the electrophoretic mobility contribution of a 3-base loop to be between that of a 2- and a 3-base-paired duplex, the mobility of a 9-base-paired duplex

Table III: Ethidium Fluorescence Lifetime Distribution in Various DNA Solutions

	τ_1 (α_1)[a]	τ_2 (α_2)	τ_3 (α_3)	$R(\chi^2)$
d(GGGGTTTGGGGTTTCCCC)	1.8 (0.189)		18.2 (0.811)	6.529
	1.8 (0.170)	7.99 (0.170)	21.7 (0.660)	1.792
d(CCCCTTTGGGGTTTGGGG)	1.8 (0.288)		12.8 (0.712)	2.839
	1.8 (0.272)	9.50 (0.416)	21.7 (0.312)	0.890
d(GGGGTTTCCCCTTTGGGG)	1.8 (0.054)		18.9 (0.947)	4.804
	1.8 (0.043)	8.39 (0.139)	21.7 (0.818)	0.636
d(GGGGTTTCCCCTTTCCCC)	1.8 (0.070)		18.8 (0.930)	11.67
	1.8 (0.056)	8.60 (0.189)	21.7 (0.755)	0.338
d(CCCCTTTGGGGTTTCCCC)	1.8 (0.059)		19.6 (0.941)	3.449
	1.8 (0.051)	9.84 (0.144)	21.7 (0.805)	0.196
d(CCCCTTTCCCCTTTGGGG)	1.8 (0.037)		20.4 (0.963)	2.108
	1.8 (0.032)	11.0 (0.111)	21.7 (0.857)	0.416

[a] τ_n values are in nanoseconds and α_n values are the corresponding fractional fluorescence intensity contributions.

is predicted for such an intramolecular triplex. This is borne out by our observation of electrophoretic mobilities in which these two oligomers are slightly faster than a decameric duplex. The formation of a single hairpin duplex with a dangling single strand in d(GGGGTTTCCCCTTTGGGG) and the C2G1 oligomers, on the other hand, will likely result in an electrophoretic mobility of 13–14-mer duplex, again consistent with our observation of a mobility significantly slower than a decamer but only slightly slower than a dodecamer duplex (not shown). The absence of discernible bands with slower electrophoretic mobilities indicates that dimeric and multimeric duplexes do not contribute significantly, possibly the consequence of energetically unfavorable duplex formation containing large bulges.

The notion of intramolecular triplex formation in d(CCCCTTTGGGGTTTGGGG) and d(GGGGTTTGGGGTTTCCCC) is further supported by the distinct hyperchromic effects and the observation of a characteristic negative CD band around 278 nm that had earlier been attributed to the G·G·C triplex formation in poly(dG)·poly(dC) (Marck & Thiele, 1978; Thiele et al., 1978). Additional supports have also come from the drug binding studies that indicate that these oligomers bind to ACTD, CHR, and EB much more weakly than d(GGGGTTTCCCCTTTGGGG) and the three C2G1 oligomers studied. This is consistent with the interpretation that the G·G·C triplexes are unfavorable for binding to these drugs. Significant binding differences, however, are found between these two weakly binding oligomers and are decidedly drug dependent. For example, C/G/G binds to ethidium somewhat weaker than G/G/C, whereas the reverse is true for the CHR binding. Although the reasons for such differences are not clear, they may have their origin in the subtle sequence-dependent conformations, differing binding modes (intercalative for EB and groove binding for CHR), and/or differing triplex to hairpin equilibria.

The unfavorable CHR binding to a triplex may be attributed to the fact that the major groove is being occupied by a DNA strand and thus is inaccessible to one of the carbohydrate side chains of this minor groove binding drug to anchor there (Banville et al., 1990). The presence of a third strand at the major groove may have also stiffened the DNA so that local duplex distortion to accommodate intercalative ligands and minor groove widening to fit the groove-binding ligand become more difficult. The much weaker drug binding ability of the G·G·C triplex as compared to the G·C duplex has also been corroborated by our experiments with poly(dG)·poly(dC) samples exhibiting strong vs no negative 278 nm CD bands (not shown). The weak EB binding of the G·G·C triplex is also in accord with the negligible ethidium fluorescence enhancement observed in some pyr·pur·pyr triplexes (Lee et al., 1979).

The strong affinities for the drugs exhibited by the other 18-mers further suggest that hairpin duplexes are good receptors for these drugs. Significant binding variations are again demonstrated by different oligomers and ligands. For example, C/C/G binds to ethidium about twice as strongly as C/G/C or G/C/C, whereas C/G/C and G/C/C binds to CHR an order of magnitude stronger than C/C/G. The dramatic reduction in the binding strength of C/C/G to CHR is particularly puzzling. The contrasting binding orders of these two drugs again suggest that factors such as differing binding modes and sequence-dependent conformations may be important. It is somewhat of a surprise that ACTD binds strongly to all three C2G1 oligomers [stronger than binding to poly(dG)·poly(dC)], with binding constants comparable to those dimeric duplexes containing the strong-binding dG-dC sequences (Chen, 1988). Another interesting aspect of the drug binding results is that the binding density obtained from Scatchard plots for ACTD is about one drug molecule per oligomeric strand, whereas more than two drug molecules are found in the case of CHR. As the 4-base-paired stem is only large enough to serve as one binding site for these extended ligands, the results are consistent with the recent NMR studies indicating that CHR binds to DNA in the form of a dimer (Gao & Patel, 1989).

Our fluorescence lifetime measurements indicate that in cases such as ethidium in which lifetimes are greatly increased upon DNA binding, lifetime analysis via dynamic measurements can be a useful technique for obtaining binding information especially when the binding strength is weak.

It should also be noted in passing that our magnesium chloride titrations indicate that the divalent cation Mg^{2+} is not essential for the intramolecular triplex formation of the G·G·C type. Our experiments with poly(dG)·poly(dC), however, did indicate that magnesium chloride somewhat facilitates intermolecular triplex formation of this type (Kohwi & Kohwi-Shigematsu, 1988).

Despite our original intention of using the C2G1 oligomers to investigate the possible intramolecular triplex formation of the C^+·G·C type, this report has concentrated mainly on the triplex formation of the G·G·C type. Such an emphasis has been necessitated by two just published reports describing the formation of intramolecular triplexes of the pyr·pur·pyr type (Sklenar & Feigon, 1990; Haner & Dervan, 1990). In this connection, it is also worth noting a most recent work on a semiintramolecular triplex structure mimicking H-DNA by a 24-mer pyrimidine strand of a "mirror" repeated sequence whose 3′-half can form an antiparallel duplex with an 11-mer purine strand (Xodo et al., 1990).

In conclusion, our results appear to demonstrate that intramolecular triple helical DNA of pur·pur·pyr type can be formed in a short oligomer via double hairpin formation. The

chief advantage of such a construct when compared to the intermolecular triplex formation is that a shorter triplex stem can be formed in a much lower DNA concentration. The design of the sequences has led to the conclusion that the two G tracts are antiparallel to each other in a G·G·C triplex, in agreement with the suggestion by Kohwi and Kohwi-Shigematsu (1988) but at variance with that of Cooney et al. (1988). However, one cannot rule out the possibility that the inability of G/C/G to form intramolecular triplex with parallel G strands may be that the T_3 loops are too short for such a conformation. In contrast to the hairpin duplexes, G·G·C triplexes appear to have low affinity for actinomycin D, chromomycin A_3, and ethidium bromide. Our demonstration of the ease in intramolecular triplex formation of the G·G·C type will greatly expand our repertoire for the duplex DNA recognition and cleavage in which only the pyr·pur·pyr triplex formation has thus far been actively pursued. In this connection, the work of Letai et al. (1988) deserves particular attention in which a full range of base specificity in the triplex formation has been investigated.

ACKNOWLEDGMENTS

I thank Ms. L. Satterfield for her technical assistance.

REFERENCES

Banville, D. C., Kenniry, M. A., Kam, M., & Shafer, R. H. (1990) *Biochemistry 29*, 6521–6534.
Broitman, S. L., Im, D. D., & Fresco, J. R. (1987) *Proc. Natl. Acad. Sci. U.S.A. 84*, 5120–5124.
Chen, F.-M. (1988) *Biochemistry 27*, 6393–6397.
Cooney, M., Czernuszewicz, G., Postel, E. H., Flint, S. J., & Hogan, M. E. (1988) *Science 241*, 456–459.
DeDoan, T., Perrouault, L., Praseuth, D., Habhooub, N., Decout, J.-L., Thuong, N. T., Lhomme, J., & Helen, C. (1987) *Nucleic Acids Res. 15*, 7749–7760.
De los Santos, C., Rosen, M., & Patel, D. (1989) *Biochemistry 28*, 7282–7289.
Elgin, S. C. R. (1984) *Nature 309*, 213–214.
Fasman, G. D., Ed. (1975) *Handbook of Biochemistry and Molecular Biology*, 3rd ed., Vol. I, p 589, CRC Press, Cleveland, OH.
Francois, J.-C., Saison-Behmoaras, T., Chassignol, M., Thuong, N. T., & Helene, C. (1989) *J. Biol. Chem. 264*, 5891–5898.
Gao, X., & Patel, D. J. (1989) *Biochemistry 28*, 751–762.
Gray, D. M., & Bollum, F. J. (1974) *Biopolymers 13*, 2087–2102.
Haner, R., & Dervan, P. B. (1990) *Biochemistry 29*, 9761–9765.
Horne, D. A., & Dervan, P. B. (1990) *J. Am. Chem. Soc. 112*, 2435–2437.
Htun, H., & Dahlberg, J. E. (1988) *Science 241*, 1791–1796.
Johnston, B. H. (1988) *Science 241*, 1800–1804.
Kohwi, Y., & Kohwi-Shigematsu, T. (1988) *Proc. Natl. Acad. Sci. U.S.A. 85*, 3781–3785.
Larsen, A., & Weintraub, H. (1982) *Cell 29*, 609–622.
Lee, J. S., Johnson, D. A., & Morgan, A. R. (1979) *Nucleic Acids Res. 6*, 3073–3091.
Lee, J. S., Woodsworth, M. L., Latimer, L. P., & Morgan, A. R. (1984) *Nucleic Acids Res. 12*, 6603–6614.
Letai, A. G., Palladino, M. A., Fromm, E., Rizzo, V., Fresco, J. R. (1988) *Biochemistry 27*, 9108–9112.
Lyamichev, V. I., Merkin, S. M., & Frank-Kamenetskii, M. D. (1986) *J. Biomol. Struct. Dyn. 3*, 667–669.
Maher, L. J., III, Wold, B., & Dervan, P. B. (1989) *Science 245*, 725–730.
Marck, C., & Thiele, D. (1978) *Nucleic Acids Res. 5*, 1017–1028.
Mosher, H. E., & Dervan, P. B. (1987) *Science 238*, 645–650.
Nickol, J. M., & Felsenfeld, G. (1983) *Cell 35*, 467–477.
Perrouault, L., Asseline, U., Rivalle, C., Thuong, N. T., Bisagni, E., Giovannangeli, C., Le Doan, R., & Helene, C. (1990) *Nature 344*, 358–360.
Pilch, D. S., Levenson, C., & Shafer, R. H. (1990) *Proc. Natl. Acad. Sci, U.S.A 87*, 1942–1946.
Povsic, T. J., & Dervan, P. B. (1989) *J. Am. Chem. Soc. 111*, 3059–3061.
Praseuth, D., Perrouault, L., Le Doan, T., Chassignol, M., Thuong, N., & Helene, C. (1988) *Proc. Natl. Acad. Sci. U.S.A. 85*, 1349–1353.
Rajagopal, P., & Feigon, J. (1989) *Biochemistry 28*, 7859–7870.
Sklenar, V., & Feigon, J. (1990) *Nature 345*, 836–838.
Strobel, S. A., & Dervan, P. B. (1990) *Science 249*, 73–75.
Strobel, S. A., Moser, H. E., & Dervan, P. B. (1988) *J. Am. Chem. Soc. 110*, 7927–7929.
Thiele, D., Marck, C., Schneider, C., & Guschlbauer, W. (1978) *Nucleic Acids Res. 5*, 1997–2012.
Umemoto, K., Sarma, M. H., Gupta, G., Luo, J., & Sarma, R. H. (1990) *J. Am. Chem. Soc. 112*, 4539–4545.
Wells, R. D., Collier, D. A., Hanvey, J. C., Shimizu, M., & Wohlrab, F. (1988) *FASEB J. 2*, 2939–2949.
Xodo, L. E., Manzini, G., & Quadrifoglio, F. (1990) *Nucleic Acids Res. 18*, 3557–3564.